

# Predicting the temperature of CRTS III ballastless tracks in cold regions based on a TCN-Track model

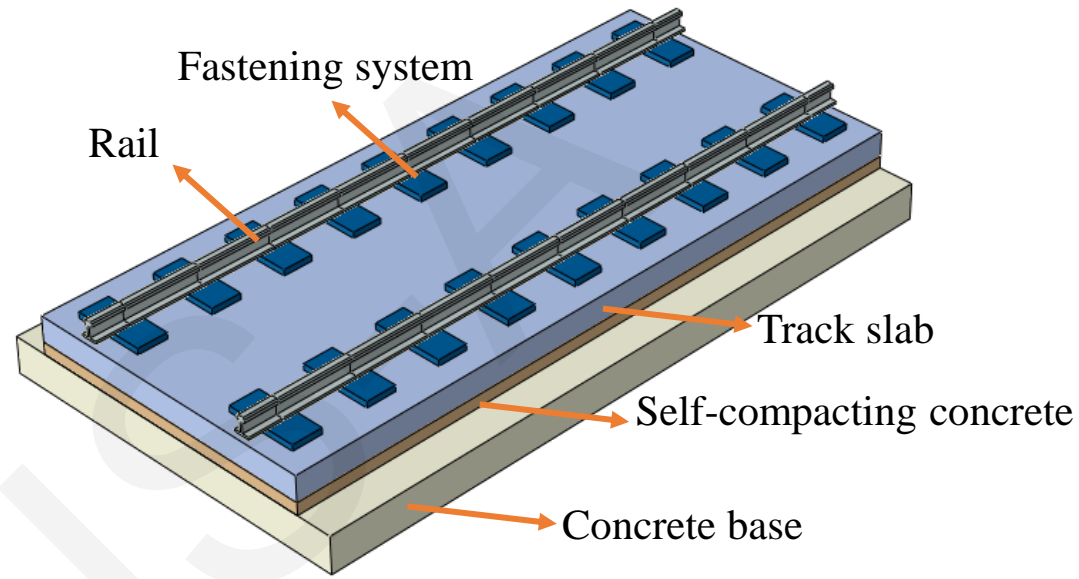
Jie LIANG, Shijie DENG, Juanjuan REN, Wenlong YE,  
Kaiyao ZHANG, Dacheng LI, Ronghe ZHANG

Cite this as: Jie LIANG, Shijie DENG, Juanjuan REN, Wenlong YE, Kaiyao ZHANG, Dacheng LI, Ronghe ZHANG, 2026. Predicting the temperature of CRTS III ballastless tracks in cold regions based on a TCN-Track model.

*Journal of Zhejiang University-SCIENCE A*, 27(1):43-57.

<https://doi.org/10.1631/jzus.A2400527>

# 1. Research subjects

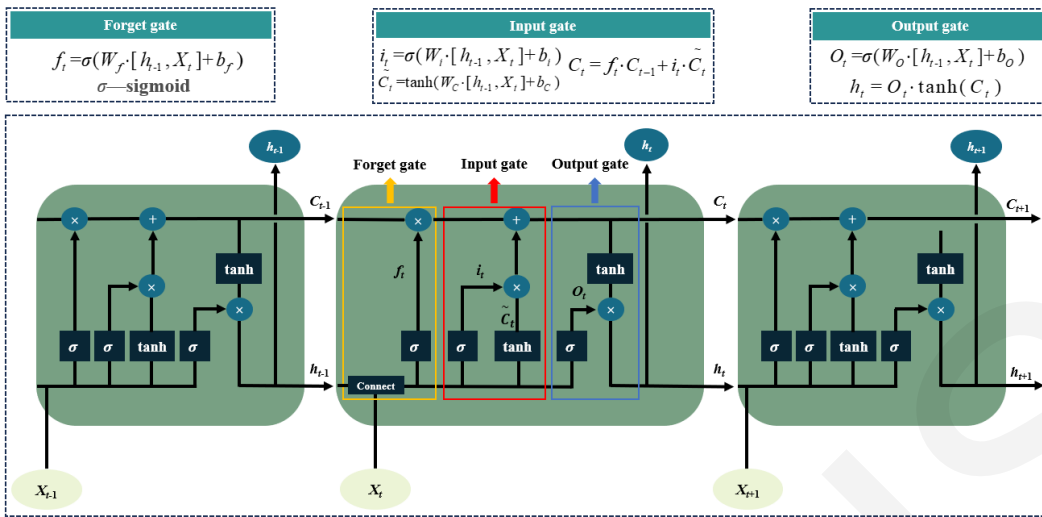


Structural composition of CRTS III prefabricated slab track

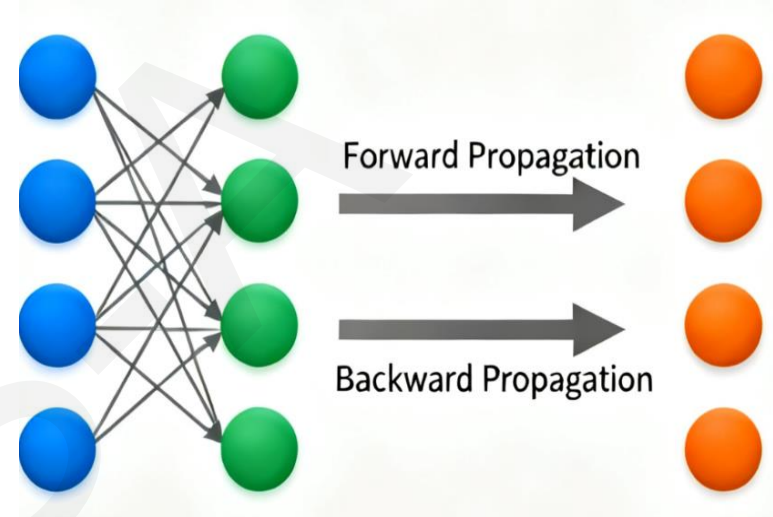


Low temperature causes damage to ballastless track

## 2. The shortcomings of traditional methods



Structure of the LSTM model

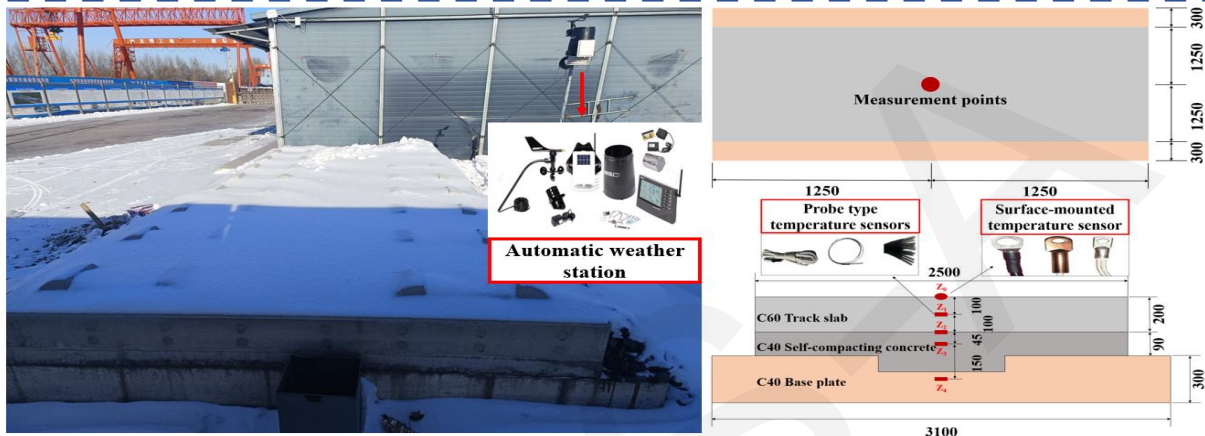


Structure of the BP model

### The shortcomings of traditional methods

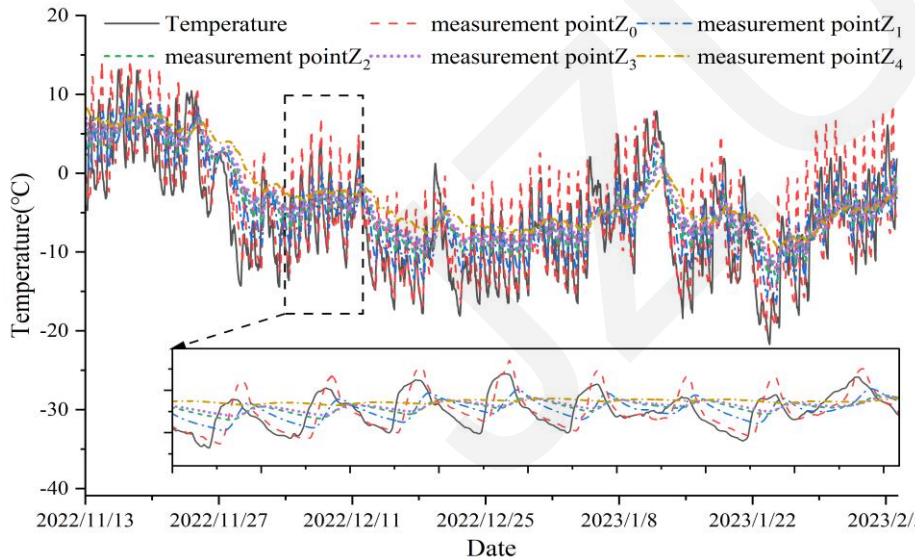
- Existing models neglect the cumulative effects of historical meteorological conditions, limiting their ability to capture long-term influences on the track temperature field.
- Mainstream temperature prediction methods focus on instantaneous values, lacking the continuity required for engineering applications.
- Most studies consider only the surface temperature of ballastless tracks, failing to represent the overall thermal behavior of the multilayer track structure.

# 3. Test plan for monitoring the temperature field of a ballastless tracks

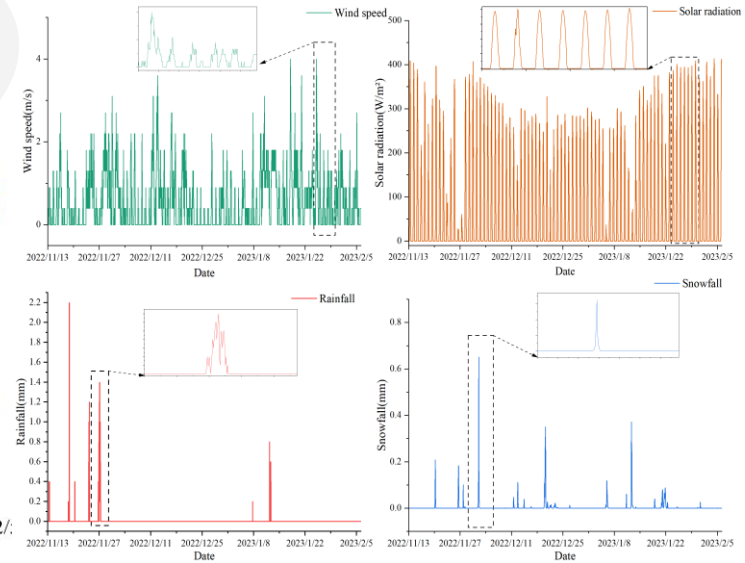


Layout of sensors for full-scale testing

obtain

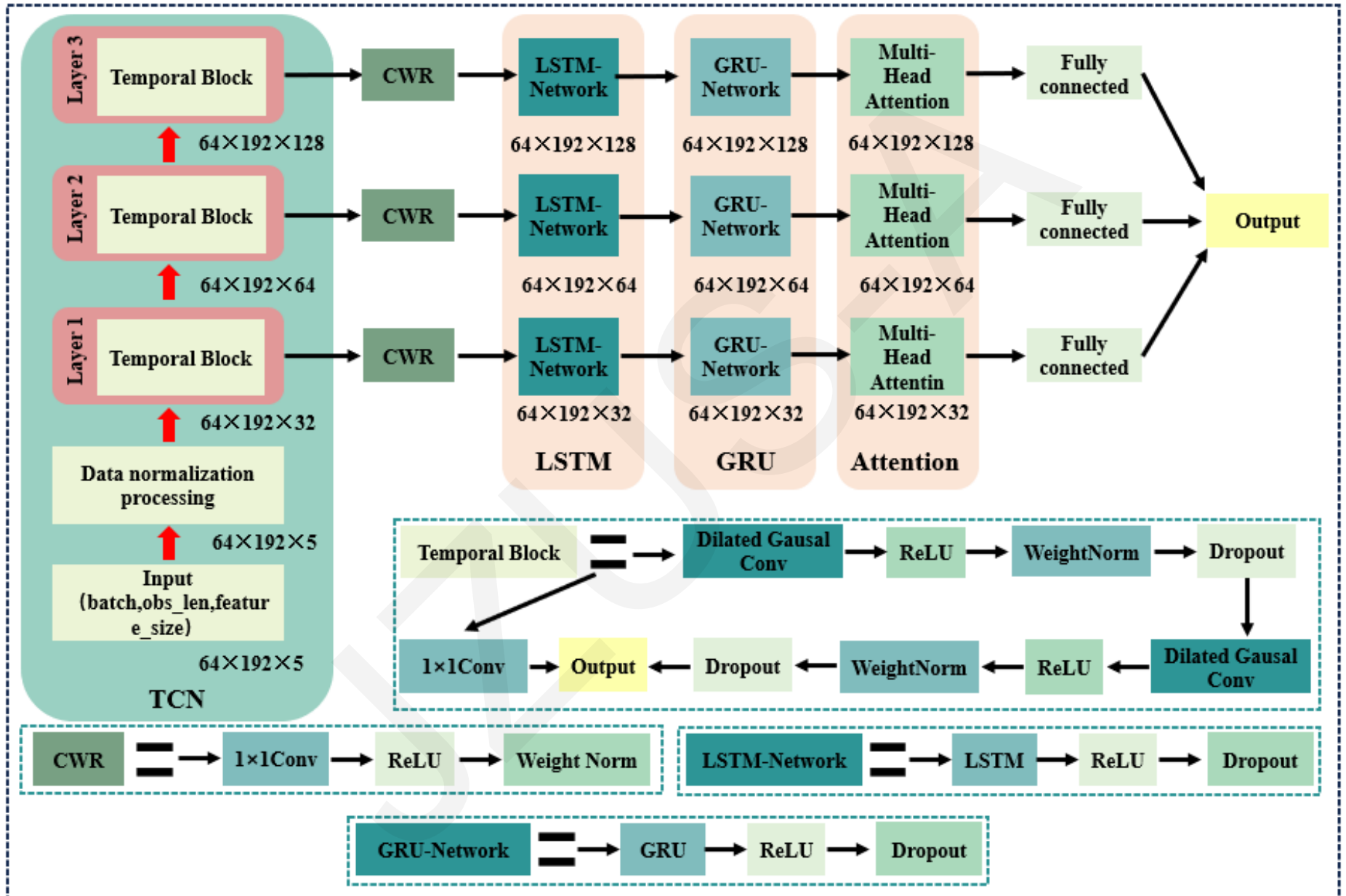


Track temperature and atmospheric temperature data



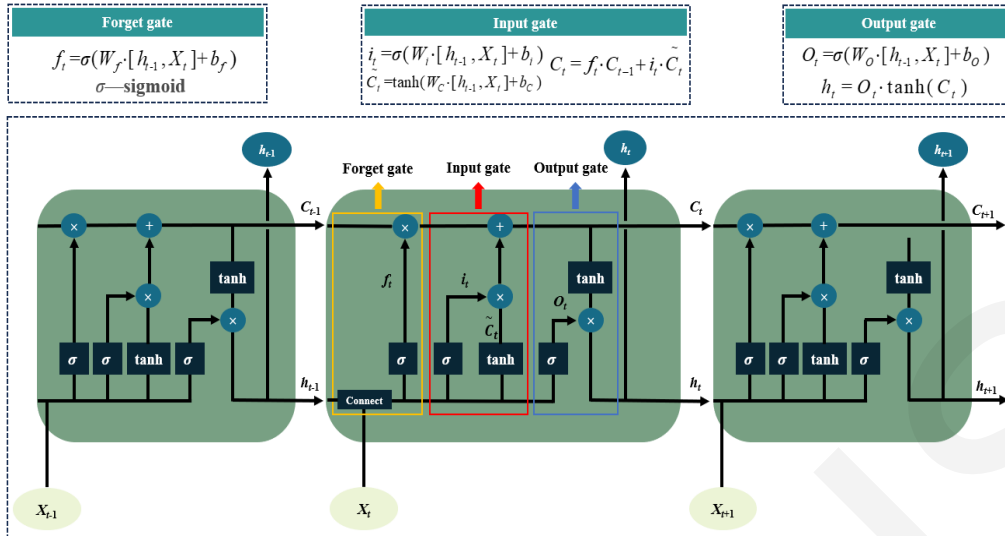
Meteorological data

# 4. Track temperature prediction model

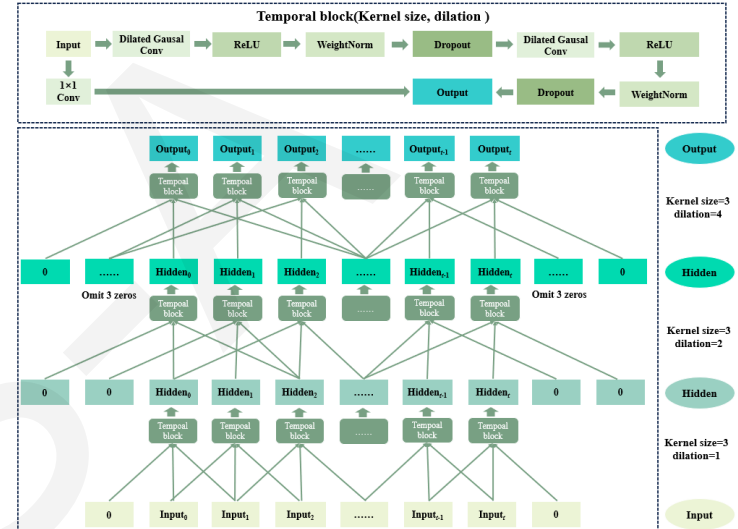


Structure of the TCN-Track model

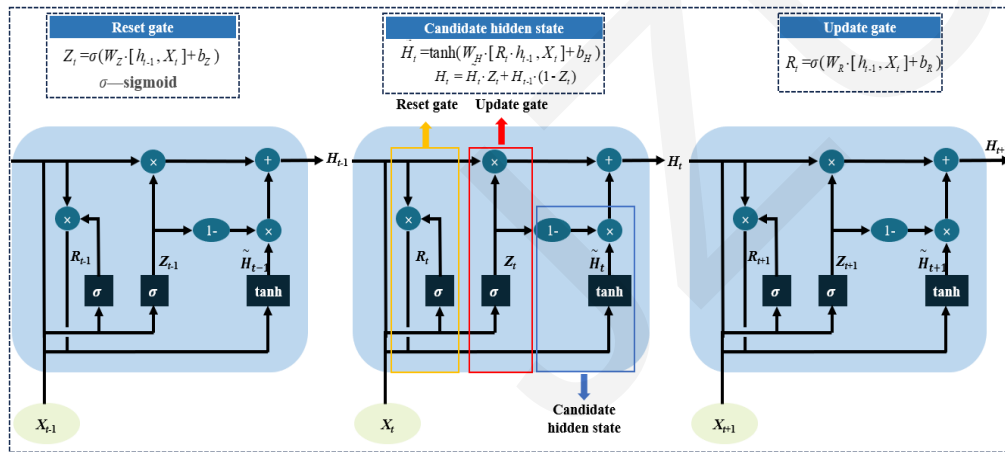
# 4. Track temperature prediction model



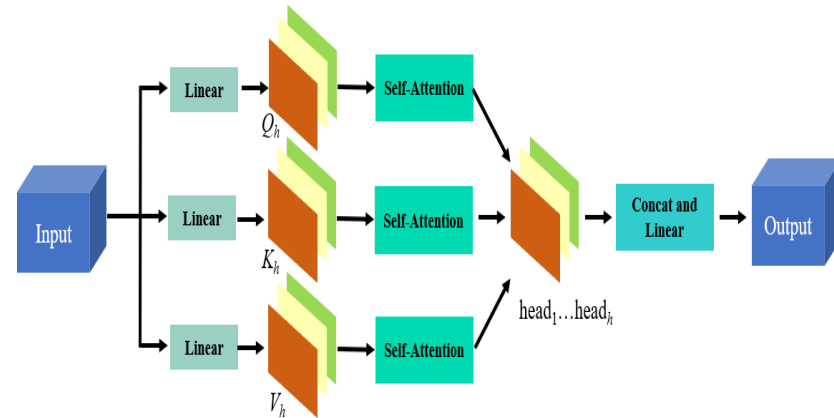
Structure of the LSTM model



Structure of the TCN model



Structure of the GRU model



Structure of the Multi-Head Attention model

# 5. Prediction results and analysis of the temperature field of the ballastless tracks

$$\text{RMSE} = \sqrt{\frac{1}{n} \sum_{i=1}^n (y_i - \hat{y}_i)^2}$$

$$\text{MAE} = \frac{1}{n} \sum_{i=1}^n |y_i - \hat{y}_i|$$

$$R = \frac{\sum_{i=1}^n (y_i - \bar{y})(\hat{y}_i - \bar{\hat{y}})}{\sqrt{\sum_{i=1}^n (y_i - \bar{y})^2 \sum_{i=1}^n (\hat{y}_i - \bar{\hat{y}})^2}}$$

## Evaluation Metrics

| Measurement point | Metrics | Epochs |              |              |              |       |
|-------------------|---------|--------|--------------|--------------|--------------|-------|
|                   |         | 100    | 150          | 200          | 250          | 300   |
| Z <sub>0</sub>    | RMSE    | 6.13   | 2.73         | 0.84         | <b>0.77</b>  | 0.81  |
|                   | MAE     | 5.69   | 2.08         | 0.69         | <b>0.62</b>  | 0.62  |
|                   | R       | 0.795  | 0.836        | 0.944        | <b>0.980</b> | 0.974 |
| Z <sub>1</sub>    | RMSE    | 5.32   | 0.89         | 0.69         | <b>0.64</b>  | 0.64  |
|                   | MAE     | 5.25   | 0.80         | 0.64         | <b>0.53</b>  | 0.58  |
|                   | R       | 0.807  | 0.939        | 0.944        | <b>0.961</b> | 0.942 |
| Z <sub>2</sub>    | RMSE    | 3.89   | 1.18         | 0.62         | <b>0.62</b>  | 0.79  |
|                   | MAE     | 3.27   | 0.93         | 0.49         | <b>0.49</b>  | 0.60  |
|                   | R       | 0.811  | 0.898        | 0.923        | <b>0.934</b> | 0.900 |
| Z <sub>3</sub>    | RMSE    | 0.69   | 0.62         | <b>0.51</b>  | 0.51         | 0.66  |
|                   | MAE     | 0.56   | 0.49         | <b>0.39</b>  | 0.42         | 0.53  |
|                   | R       | 0.872  | 0.881        | <b>0.888</b> | 0.884        | 0.875 |
| Z <sub>4</sub>    | RMSE    | 0.36   | <b>0.32</b>  | 0.39         | 0.43         | 0.86  |
|                   | MAE     | 0.36   | <b>0.32</b>  | 0.36         | 0.36         | 0.80  |
|                   | R       | 0.829  | <b>0.839</b> | 0.834        | 0.830        | 0.807 |

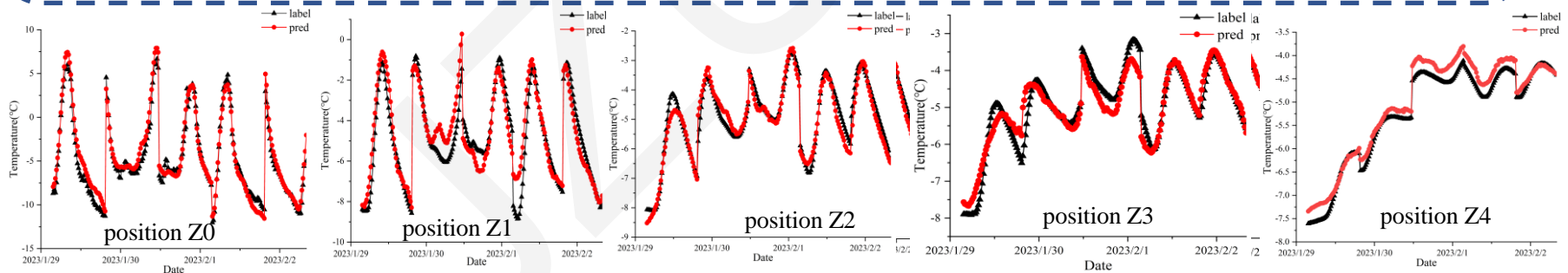
## Prediction results of different epochs

- The optimal training epoch for the TCN-Track model was found to be 250, balancing prediction accuracy and overfitting risk.
- Deeper track layers exhibited more stable and accurate temperature predictions, as their pronounced thermal variations enhanced the model's learning efficiency.
- Excessive epochs led to performance degradation, indicating potential overfitting.

# 5. Prediction results and analysis of the temperature field of the ballastless tracks

| Measurement point | Metrics | Kernel size |              |              |       |              |
|-------------------|---------|-------------|--------------|--------------|-------|--------------|
|                   |         | 3           | 6            | 9            | 12    | 15           |
| $Z_0$             | MAE     | 0.62        | 0.49         | <b>0.39</b>  | 0.48  | 0.46         |
|                   | RMSE    | 0.77        | 0.61         | <b>0.50</b>  | 0.59  | 0.57         |
|                   | R       | 0.965       | 0.978        | <b>0.985</b> | 0.984 | 0.984        |
| $Z_1$             | MAE     | 0.53        | 0.45         | <b>0.38</b>  | 0.48  | 0.45         |
|                   | RMSE    | 0.64        | 0.55         | <b>0.47</b>  | 0.58  | 0.53         |
|                   | R       | 0.961       | 0.968        | 0.974        | 0.981 | <b>0.982</b> |
| $Z_2$             | MAE     | 0.49        | 0.46         | <b>0.37</b>  | 0.39  | 0.39         |
|                   | RMSE    | 0.62        | 0.56         | <b>0.45</b>  | 0.47  | 0.46         |
|                   | R       | 0.934       | 0.910        | 0.931        | 0.926 | <b>0.955</b> |
| $Z_3$             | MAE     | 0.42        | 0.38         | <b>0.34</b>  | 0.39  | 0.39         |
|                   | RMSE    | 0.51        | 0.47         | <b>0.42</b>  | 0.48  | 0.48         |
|                   | R       | 0.884       | <b>0.918</b> | 0.895        | 0.839 | 0.878        |
| $Z_4$             | MAE     | 0.36        | 0.30         | 0.26         | 0.25  | 0.30         |
|                   | RMSE    | 0.43        | 0.34         | <b>0.32</b>  | 0.31  | 0.36         |
|                   | R       | 0.830       | 0.837        | <b>0.888</b> | 0.861 | 0.850        |

Prediction results of different convolutional kernel sizes



Temperature prediction results of different measuring points

- The convolution kernel size of 9 provides the best overall performance, achieving a balance between local feature extraction and global information capture.
- Smaller kernels limit the receptive field, while larger ones increase parameters and lead to overfitting.

# 5. Prediction results and analysis of the temperature field of the ballastless tracks

| Algorithm | Metrics | Measurement point |                |                |                |                |
|-----------|---------|-------------------|----------------|----------------|----------------|----------------|
|           |         | Z <sub>0</sub>    | Z <sub>1</sub> | Z <sub>2</sub> | Z <sub>3</sub> | Z <sub>4</sub> |
| GRU       | MAE     | 3.51              | 2.46           | 1.48           | 1.08           | 1.00           |
|           | RMSE    | 4.12              | 2.92           | 1.74           | 1.32           | 1.08           |
|           | R       | 0.77              | 0.851          | 0.86           | 0.722          | 0.767          |
| TCN       | MAE     | 2.49              | 1.81           | 1.50           | 1.34           | 1.31           |
|           | RMSE    | 3.20              | 2.20           | 1.69           | 1.49           | 1.35           |
|           | R       | 0.782             | 0.686          | 0.872          | 0.700          | 0.704          |
| LSTM      | MAE     | 3.60              | 1.56           | 1.29           | 1.59           | 1.15           |
|           | RMSE    | 4.35              | 1.96           | 1.56           | 1.79           | 1.31           |
|           | R       | 0.833             | 0.732          | 0.821          | 0.710          | 0.704          |
| TCN-LSTM  | MAE     | 1.80              | 1.12           | 0.90           | 0.35           | 0.28           |
|           | RMSE    | 2.14              | 1.34           | 1.00           | 0.45           | 0.35           |
|           | R       | 0.922             | 0.914          | <b>0.962</b>   | 0.826          | 0.866          |
| TCN-GRU   | MAE     | 1.44              | 1.36           | 0.91           | 0.67           | 0.58           |
|           | RMSE    | 1.82              | 1.71           | 1.10           | 0.82           | 0.65           |
|           | R       | 0.938             | 0.937          | 0.904          | 0.882          | 0.821          |
| GRU-LSTM  | MAE     | 2.29              | 1.71           | 1.32           | 1.49           | 0.73           |
|           | RMSE    | 2.91              | 2.05           | 1.53           | 1.64           | 0.81           |
|           | R       | 0.901             | 0.911          | 0.908          | 0.832          | 0.798          |
| TCN-Track | MAE     | <b>0.39</b>       | <b>0.38</b>    | <b>0.37</b>    | <b>0.34</b>    | <b>0.26</b>    |
|           | RMSE    | <b>0.50</b>       | <b>0.47</b>    | <b>0.45</b>    | <b>0.42</b>    | <b>0.32</b>    |
|           | R       | <b>0.985</b>      | <b>0.974</b>   | 0.931          | <b>0.895</b>   | <b>0.888</b>   |

## Model comparison

- The TCN-Track model outperforms six benchmark time-series prediction models across all evaluation metrics (MAE, RMSE, and R).
- Compared with other models, it achieves a 3.61%–89.17% reduction in MAE, a 6.67%–88.51% reduction in RMSE, and a 1.45%–29.57% increase in correlation coefficient (R).
- Although slightly lower than the TCN-LSTM model at one measurement point (Z<sub>2</sub>, R = 0.931), the overall performance demonstrates superior prediction accuracy and generalization capability.

## 6. Conclusions

- The on-site measured data from the Shenyang area were systematically analyzed across time and space dimensions, exploring the effects of temperature, solar radiation, wind speed, rainfall, and snowfall on the track temperature field.
- The TCN-Track model incorporates the cumulative effects of meteorological factors and improves feature extraction by merging TCN, LSTM, and GRU models with a multi-head attention mechanism, achieving precise temperature predictions for multi-layer track structures. The model predicts the daily temperature for each layer of the ballastless tracks structure with an MAE between 0.26 and 0.39, an RMSE between 0.32 and 0.50, and an R between 0.888 and 0.985.
- Compared to models like TCN, LSTM, and GRU for predicting track temperature fields, the TCN-Track model reduced the MAE by 3.61% to 89.17%, reduced the RMSE by 6.67% to 88.51%, and increased R by 1.45% to 29.57%.